PHYSICAL REVIEW C VOLUME 6, NUMBER 3 SEPTEMBER 1972

Fission Barriers for Nuclei Lighter than Radium*

Ulrich Mosel
Physics Department, University of Washington, Seattle, Washington 98195
(Received 21 April 1972)

Potential energy surfaces have been calculated for the mass range $180 \leq A \leq 212$ by using the shell-correction method on the basis of a symmetric two-center shell model. All calculations have been performed both with a constant and with a surface-dependent pairing strength. The results show that the fission barriers calculated with the latter prescription are incompatible with experimental data. The calculations for a constant pairing strength, however, in which the shells at the saddle are calculated on the same basis as those at the ground state, agree reasonably well with experimental data of the Berkeley group. The shell corrections for these nuclei are analyzed separately in detail and are found to exhibit remarkable regular structures which can be explained by an interplay between the shells of the fragments and those of the fissioning nucleus. Finally, the existence of shape-isomeric states and the treatment of the zero-point energy in these calculations are discussed.

I. INTRODUCTION

In recent years a large number of calculations of potential energy surfaces (PES) in heavy nuclei has been reported.[1,2] Nilsson *et al.* have published a thorough and complete survey of saddle-point properties of the actinides by using an extended Nilsson model[1] in combination with the Strutinsky prescription.[2] This model is suitable for the description of nuclear shapes that can be described essentially as small distortions of spheroidal shapes as they are encountered between the ground state and the saddle point in the actinides and superheavy nuclei. In these regions the calculations of Nilsson *et al.* and later on also other groups[2] have contributed substantially to the understanding of the systematic behavior of shell effects between the ground state and the saddle point.

As has been pointed out, however, some time ago,[3] the center point of the Nilsson potentials remains the deepest point of the potential, even for distortions that correspond to the development of a considerable constriction.[4] This property makes it impossible to describe with these potentials shapes that are highly constricted, e.g. those which are encountered on the path between saddle and scission in heavy nuclei and already at the saddle point in lighter elements ($A \lesssim 200$).

The recently developed two-center model (TCM) avoids these restrictions.[5] In this model it is possible to describe the Nilsson potentials (one-center potentials) as well as configurations of two completely separated fragment nuclei with their correct asymptotic shell structure. The effects of shells of the fissioning nucleus can thus be treated on the same basis as those of shells of the fragment nuclei.

This model has already been applied to a thorough investigation of the effects of fragment shells in the actinide and Pb region.[6,7] It was the main concern in Ref. 7 to investigate systematically the behavior of fragment shell influences in heavy nuclei over a wide mass range rather than to study in a very detailed manner the properties of specific nuclei. Such a study was also prohibited by the restriction to symmetric nuclear shapes which are not appropriate for a detailed investigation of potential energy surfaces in the heavy-element region where asymmetric fission prevails at low excitation energies.

The elements with masses $A \lesssim 226$ are known, however, to fission symmetrically. Since calculations in an extended Nilsson model are not able to describe the highly constricted saddle points in this region and since only very few and incomplete theoretical results have been reported for this area[7,8] so far, it is worthwhile to do more systematic calculations over a larger range of masses. This paper, therefore, contains the results of calculations of fission barriers for 20 nuclei in the mass region $180 \leq A \leq 212$. A first short note on these calculations already has been published elsewhere.[9]

We will show two-dimensional PES's for these nuclei in comparison with the liquid-drop model (LDM) predictions and discuss the differences between the predictions of these two models. We will also specifically analyze the influence of the pairing interaction on the PES's. It is hoped that this study will thus contribute to the rather important question if the pairing force should be made surface-dependent. Because of their larger constrictions, and thus also larger surface areas, fission barriers in lighter elements are much more suitable for an investigation of this problem than those of heavy elements. It is hoped to get

some insight into this question from a comparison of fission barriers and BCS gap parameters at the saddle obtained in calculations both with and without a surface dependence of the pairing strength.

The shell corrections alone will the be specifically analyzed. It will be shown that these quantities contain regular structures in deformation space. The reasons for this behavior will be discussed, especially in connection with the transition from compound nucleus to fragment shells.

Finally we will address ourselves to the question of the existence of shape-isomeric structures in fission of lighter elements as well as to the problem of nuclear zero-point energies and their influence on potential energy surfaces.

II. TWO-CENTER MODEL

Since the mathematical details of the model have already been published,[5,6] we restrict ourselves here to a short review of its basic properties. The Hamiltonian of the model is given by

$$H = T + \frac{m}{2}\omega_\rho^2\rho^2 + \frac{m}{2}\omega_z^2(|z|-z_0)^2 + V_{\rm corr}(z) + V(\vec{l},\vec{s}) \ , \tag{1}$$

where $V(\vec{l},\vec{s})$ is defined as a direct generalization of the Nilsson model:

$$V(\vec{l},\vec{s}) = \begin{cases} C(z_0)\vec{l}_1\cdot\vec{s} + D(z_0)[\vec{l}_1^{\,2} - \frac{1}{2}N(N+3)] & z>0 \\ C(z_0)\vec{l}_2\cdot\vec{s} + D(z_0)[\vec{l}_2^{\,2} - \frac{1}{2}N(N+3)] & z<0 \ . \end{cases} \tag{2}$$

In Eq. (2) $\vec{l}_1$ and $\vec{l}_2$ are the two pseudoangular momenta with respect to the two centers at $z=z_0$ and $z=-z_0$, respectively (for their definition see Ref. 7). The dependence of C and D on z_0 and the definition of the N-dependent term in (2) agree with those of Ref. 6.

The parameters C and D depend as usual on the Nilsson parameters κ and μ. Their values in the present calculation are given in Table I.[1,10] The term $V_{\rm corr}$ in (1) is the same as in Ref. 7 and achieves a smoothing of the nuclear shape in the neck region

$$V_{\rm corr}(z) = -\frac{m}{2}\omega_z^2\frac{1}{2z_0^2}(|z|-z_0)^4\theta(z_0-|z|), \tag{3}$$

where θ is a step function [$\theta(x)=0$ for $x<0$, $\theta(x)=1$ for $x>0$].

For all further details of the Hamiltonian, we refer the reader to Refs. 6 and 7 and for the details of its diagonalization to Scharnweber *et al.*[5]

The single-particle levels have been calculated only once for a nucleus with the mass $A=204$ and the oscillator constant $\hbar\mathring{\omega}_0 = 41\times(204)^{-1/3}$ MeV. The use of these levels for nuclei down to $A=180$ corresponds for this nucleus to the use of a constant of 39.3 instead of 41 for the calculation of $\hbar\mathring{\omega}_0$, which is still reasonable. Otherwise this use of the same levels introduces an error of $\approx$0.5 MeV in the saddle energy of ^{180}W as has been checked by an independent calculation with levels corresponding to $A=180$ and $\hbar\mathring{\omega}_0 = 41\times(180)^{-1/3}$ MeV.

For the BCS treatment of the pairing force we have taken Z levels for the protons and N levels for the neutrons into account. The strengths have been chosen such as to reproduce the empirical odd-even mass differences at the ground state (Malov, Soloviev, and Khristov[10]). The values of G which give a good fit to these quantities are (in MeV):

$$\begin{aligned} G_p &= [20.8 - 0.0933(A-180)]/A \ ; \\ G_n &= [14.5 - 0.0233(A-180)]/A \ . \end{aligned} \tag{4}$$

Only for the $Z=74$ isotopes a different proton strength has been used: $G_p = 19.5/A$ MeV. We have performed calculations both for the case of constant and of surface-dependent pairing strengths. In the latter case the quantities in (4) have been multiplied by a shape factor B_s which gives the nuclear surface in units of that of the corresponding spherical shape.

The pairing energy itself has then been determined under the assumption that only the diagonal matrix elements at the spherical shape are included in the LDM. No further renormalization has been made. Thus $E_{\rm p}$ is given by

$$E_{\rm p} = \sum_{p,n}\left[2\sum_{\nu}^{\nu_F}\epsilon_\nu v_\nu^2 - \frac{\Delta^2}{G} - \sum_{\nu}^{\nu_F}\epsilon_\nu + \sum_{\nu}^{\nu_F}(G-G_0)\right], \tag{5}$$

where the last two summations run only over occupied states, and G_0 is the pairing strength at the spherical state.

The total PES, $E_{\rm DEF}$, is then given by

$$E_{\rm DEF} = E_{\rm LDM} + \delta U + E_{\rm p} \ . \tag{6}$$

TABLE I. The table lists the single-particle parameters κ and μ for protons and neutrons for the mass region $180 \le A \le 212$ and for the fragment region $A \approx 100$. They are, except for very small changes, taken from Nilsson *et al.* (Ref. 1) for the compound-nucleus region and from Arseniev, Sobiczewski, Soloviev (Ref. 10) for the fragment region.

	Protons		Neutrons	
Mass region	κ	μ	κ	μ
$A\approx100$	0.0688	0.558	0.0638	0.491
$A\approx200$	0.0610	0.626	0.0636	0.370

Here δU is the shell correction calculated by using the Strutinsky prescription[2] with a correction polynomial of sixth order and a smearing width of $\gamma = 1.2\hbar\mathring{\omega}_0$. The LDM energy E_{LDM} has been calculated for a drop whose shape coincides with that of the equipotential surface of (1). The parameters of Myers and Swiatecki[11] have been used.

As in Ref. 7 we have transformed the two independent shape parameters in (1) into two more imaginative quantities [the third parameter in (1) can be eliminated by using a volume conservation requirement for that equipotential surface that coincides with the nuclear surface]. These are an elongation parameter l and a constriction parameter d, defined by

$$l = \frac{z_0 + c}{R_0}, \qquad d = 1 - \frac{d_0}{a} = 1 - \left(1 - \frac{z_0^2}{2c^2}\right)^{1/2}, \tag{7}$$

where R_0 is the radius of the fissioning nucleus ($R_0 = r_0 A^{1/3}$) and c and a are defined by

$$c = \frac{\mathring{\omega}_0}{\omega_z} R_0, \qquad a = \frac{\mathring{\omega}_0}{\omega_\rho} R_0, \qquad \hbar\mathring{\omega}_0 = 41 \times A^{-1/3}\ \mathrm{MeV}\ . \tag{8}$$

Thus l gives directly the length of the nuclear shape in units of the radius of the fissioning nucleus. The constriction parameter d is a measure for the relative neck thickness with d_0 being the radius of the nuclear neck.

In the following sections we will thus discuss the PES in a two-dimensional representation, giving E_{DEF} as a function of l and d.

III. POTENTIAL ENERGY SURFACES

A. Ground-State Deformation and Shell Corrections

The ground-state deformations obtained from these calculations can be directly compared with experimental information on nuclear quadrupole moments and ground-state masses. The low single-particle level density at the Fermi surface around the double magic nucleus ^{208}Pb leads in this region to strongly negative shell corrections at zero deformation and thus spherical ground states. With decreasing proton and neutron numbers, the nuclei become softer at their ground state according to these calculations until finally below mass $A \approx 190$ the first deformed shell is populated. This behavior is in agreement with the experimental results as could be expected, since all ground-state deformations have the constriction parameter $d = 0$, i.e., can be described by a pure Nilsson model without a center separation. It is well known that the Nilsson model gives a very satisfactory description of ground-state deformations in the rare earths and actinides.[12]

The comparison of calculated ground-state shell corrections with experimental results, however, is not so straightforward. The ground-state shell correction is defined as the deviation of a measured mass from its average value, i.e. its prediction by a macroscopic mass law, like the LDM. The "experimental" shell correction thus depends on the macroscopic mass law used. A consistent comparison of "experimental" and theoretical shell corrections, therefore, necessitates a refit of the LDM to the experimental masses with the inclusion of the calculated shell corrections (sum of δU and E_{p}). The experimental corrections could then be extracted from the data by taking the difference between the measured masses and the LDM determined in this way.

This procedure, however, is rather involved. We have, therefore, restricted ourselves here to taking as "experimental" shell corrections the quantities extracted from experimental masses by Myers and Swiatecki,[11] and therefore use the term "experimental" only in quotation marks.

In a comparison of these numbers with the calculated ones, one then has to bear in mind that the "experimental" shell corrections may still contain contributions from a background that varies smoothly with nucleon numbers. There are indeed indications that the Myers and Swiatecki mass formula implicitly contains shell contributions in its LDM part (see Sec. III B for a discussion of this point).

Keeping all these reservations in mind, we compare in Fig. 1 the "experimental" and the theoretical ground-state energy shell corrections. (In the following we will consistently use the term, energy shell corrections, for the *total* contribu-

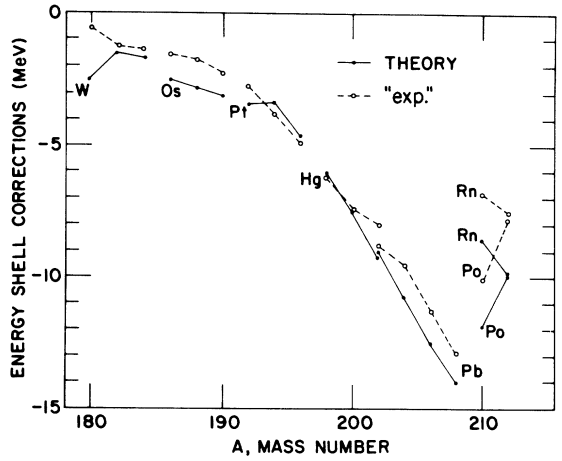

FIG. 1. The calculated ground-state shell corrections ($\delta U + E_{\mathrm{p}}$) (solid lines) are compared with the "experimental" values of Myers and Swiatecki (Ref. 11).

tion of single-particle properties to the nuclear mass, i.e., for the term $\delta U + E_p$; δU alone will be called the shell correction as usual.) Although the over-all dependence of the calculated quantities on Z and N compares well with the "experimental" numbers there are some remarkable deviations. The calculated numbers tend to overestimate the experimental ones practically in all cases, the largest difference appearing at the lower and upper boundary of the mass range investigated.

At the lower boundary around ^{180}W one finds experimentally already a rather well-developed rotational structure in the low-energy spectrum of these nuclei.[13] This means that these nuclei must have a stable ground-state deformation and thus a rather steep minimum in their deformation energy at the ground state. Although the depth of this minimum is determined by the relative size of the shell corrections at the spherical shape and at the ground state, the value derived in Ref. 11 of only −0.5 MeV for ^{180}W seems to be too small and to underestimate the true ground-state correction. Here the observed difference can thus possibly be attributed to the "experimental" numbers.

The situation seems to be different, however, at the upper end of the mass range investigated here around the element Po. There the theoretical numbers are too high in absolute value as is indicated by an analysis of the calculated fission barriers in this region (see Sec. III B).

In these comparisons it has been assumed that the calculated energy of the ground-state minimum already contains the quantum mechanical zero-point energy which thus may not be added to the calculated energy surface at the ground state (for a discussion of this point see Sec. IV).

B. Fission-Barrier Heights, G = const.

In order to illustrate the general features of PES's calculated in the model described in Sec. II, we show in Figs. 2–4 some typical examples in comparison with the pure LDM prediction. The most dominant effect of the inclusion of shell effects into the PES's is the change of the structure of the PES near the ground state of the nucleus. This is a consequence of the specific shell structure in the region considered, i.e., of the change from deformed nuclei at $A = 180$ through the transition region at $A \approx 190$–200 to the doubly magic nucleus ^{208}Pb with its very strong negative shell correction. These strong shell effects lead consequently also to strongly shell-dependent fission-barrier heights, since these are measured relative to the ground state. Based on this observation, Myers and Swiatecki[11] indeed tried to reproduce the fission barriers in this mass region by assuming shell contributions to the barrier height only at the ground state. This assumption, however, has become questionable with the discovery of large structures, e.g. second minima, in the fission barriers of the actinides. We will, therefore, in a later section specifically analyze the shell contributions to the barrier energies and try

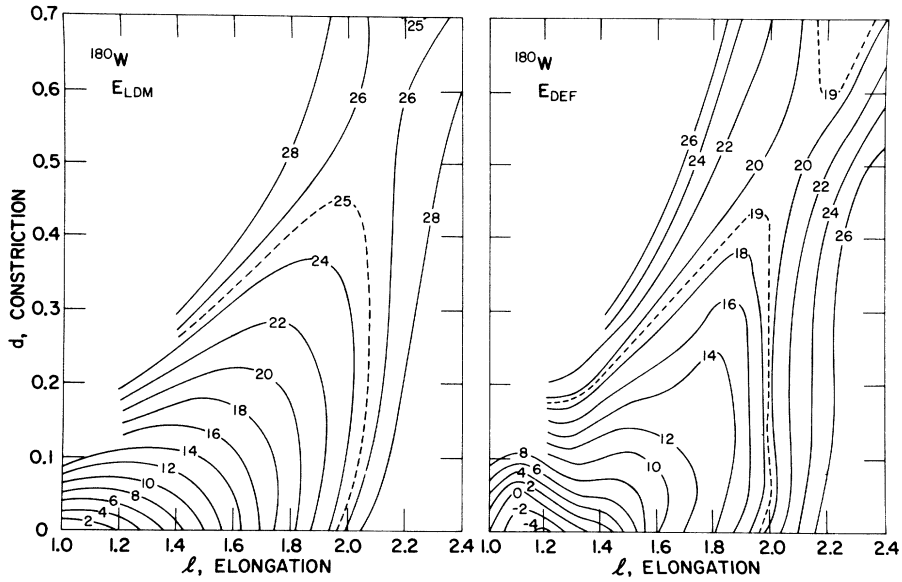

FIG. 2. The calculated PES (right side) is shown in comparison with the corresponding LDM (left side) prediction for the nucleus ^{180}W. The PES's are calculated under the assumption of a constant pairing strength. Full contour lines are drawn for an energy increase of 2 MeV. The numbers at the lines give the energies in MeV. The E_{DEF} surfaces are normalized to zero at $d = 0$, $l = 1$.

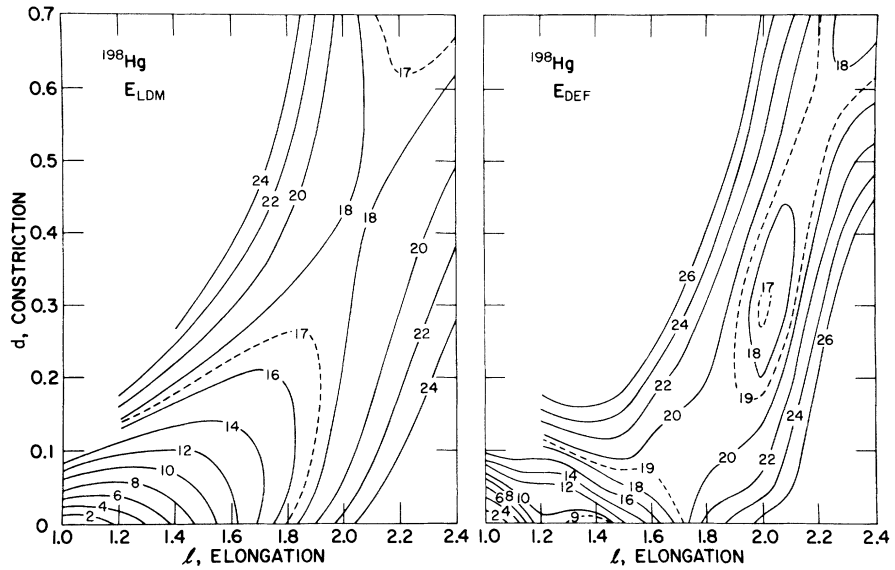

FIG. 3. The calculated PES (right side) is shown in comparison with the corresponding LDM prediction (left side) for the nucleus ^{198}Hg. For all other details see the caption of Fig. 2.

to decompose them into contributions from the ground state and the saddle.

The calculated barrier energies defined here as the difference between the calculated saddle point and the ground-state energy *without* subtraction of a zero-point energy contribution (see Sec. IV) are compiled in Table II and compared with the experimental values[14] in Fig. 5. The calculated barriers are seen to *under*estimate the experimental barriers for $A < 200$ and to overestimate them for $A \approx 210$ thus introducing a smaller decrease of the fission barriers with mass (ground-state shell effects subtracted) than is experimentally observed. The too high barriers around Po may be a consequence both of the too large calculated ground-state shell correction there and of an insufficient parametrization for the nuclear shape. Since these barriers contain the very strong shell effect at the ground state connected with the double-magic nucleus ^{208}Pb, we plot in Fig. 6 the quantity $E_B - E_0$, i.e., the difference between the barrier height and the ground-state energy shell correction.

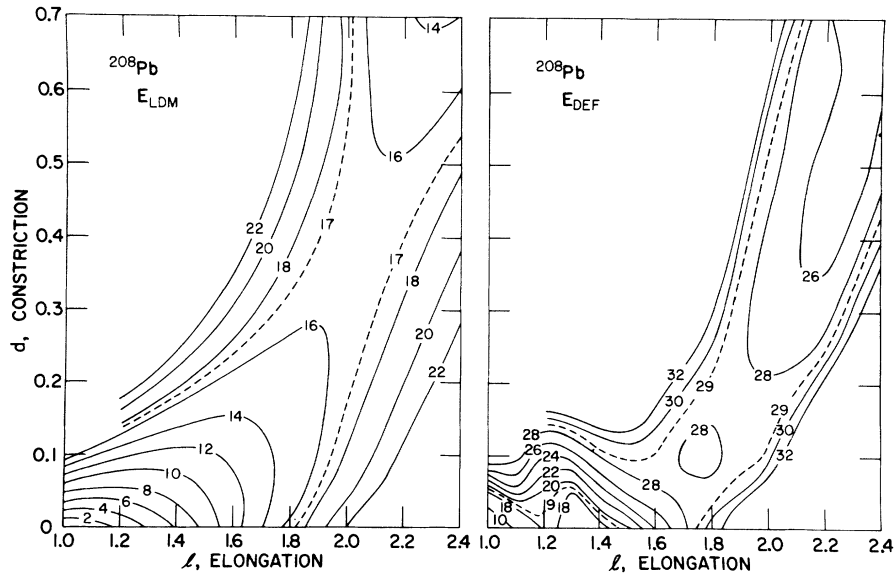

FIG. 4. The calculated PES (right side) is shown in comparison with the corresponding LDM prediction (left side) for the nucleus ^{208}Pb. For all other details see the caption of Fig. 2.

It is seen that except for $Z > 84$ all calculated barriers are *lower* than the LDM prediction for the shapes used by about 2–5 MeV. Part of this discrepancy can be understood by observing that the mass formula used[11] has been fitted to reproduce the experimental barrier height of ^{201}Tl. This fit has been performed under the assumption of no single-particle corrections at the barrier. Even if the model of a homogeneous level distribution at the saddle with a corresponding vanishing shell correction δU is accepted for the moment, these levels, however, will still lead to a pairing energy. In Table II the pairing energies $E_{p,sp}$ at the saddle point are listed for all nuclei considered here. They are found to be of the order of −2 MeV. Since these numbers are added to the LDM barrier, it is to be expected that the resulting total fission barriers will be too low, since the LDM alone already gives by construction the right value.

Part of the discrepancy is, of course, also due to the existence of sizable shell corrections δU at the saddle. These corrections are usually negative for $A \lesssim 200$ (see Table II), thus lowering the saddle-point energy and possibly shifting it away from its LDM position. This latter effect is clearly seen in Figs. 2–4 which show that for nuclei above ^{196}Pt the shell-corrected saddle lies at remarkably smaller deformations (mainly smaller constrictions) than the LDM saddle.

It may seem that this shift to smaller deformations is incompatible with experimental information on the moment of inertia at the saddle which can be described rather adequately with LDM shapes. However, it has been shown that this same effect appears in the actinides too, where the LDM saddle shapes lead to better moments of inertia in comparison with experimental results than the shapes corresponding to the shell-corrected saddle.[15] The explanation for this behavior is that shell effects tend to wash out rather soon with excitation energy so that the experimental measurements of fission anisotropies performed at rather high excitation, are indeed sensitive only to the LDM saddle.[15]

In order to understand some properties of the negative shell corrections at the saddle, the total energy shell correction is shown in Fig. 7 in comparison with the total PES for the case of ^{200}Hg (Fig. 8). One sees that at nonzero constrictions the $\delta U + E_p$ surface is dominated by a ridge of about 15-MeV height perpendicular to the l axis and a valley nearly parallel to the ridge at $l \approx 2.0$.

TABLE II. The table lists the BCS gap parameters Δ_p and Δ_n for protons and neutrons at the ground state (gs). These can directly be compared with the experimental quantities given by Malov, Soloviev, and Khristov (Ref. 10). The total ground-state energy shell correction ($\delta U + E_p$) is denoted by E_0. The barrier heights E_B are given both for a constant and a surface-dependent pairing strength G. The next column lists the shell corrections δU at the saddle point (sp) as obtained in the calculations with a constant pairing strength G. In the last column the pairing energies E_p at the saddle point (sp) as obtained with a constant G are listed for all nuclei. All energies are given in MeV.

Z	A	$\Delta_{p,gs}$	$\Delta_{n,gs}$	E_0	$G=c$ E_B	$G\sim S$ E_B	$G=c$ δU_{sp}	$G=c$ $E_{p,sp}$
74	180	0.87	0.71	−2.7	24.2	18.8	−0.3	−2.3
74	182	0.80	0.88	−1.4	24.3	18.6	−0.2	−2.6
74	184	0.80	0.86	−1.8	24.6	19.3	−0.9	−2.6
76	186	0.80	0.80	−2.5	21.2	17.0	−2.4	−1.4
76	188	0.73	0.77	−2.8	21.4	17.7	−3.3	−1.1
76	190	0.66	0.73	−3.1	21.7	18.4	−4.2	−0.8
78	192	0.66	0.70	−3.4	18.7	15.8	−3.0	−1.6
78	194	0.67	0.85	−3.3	19.2	16.6	−3.9	−1.2
78	196	0.63	0.77	−4.6	20.7	18.5	−1.5	−1.5
80	198	0.49	0.74	−6.0	19.3	18.7	−2.1	−1.4
80	200	0.46	0.64	−7.5	21.4	20.6	−2.1	−1.2
80	202	0.43	0.52	−9.2	23.1	22.7	0.2	−1.6
82	202	0.03	0.61	−9.0	21.1	21.0	1.3	−2.1
82	204	0.0	0.49	−10.7	24.0	23.1	−0.1	−1.9
82	206	0.0	0.27	−12.5	26.2	25.2	0.2	−1.9
82	208	0.0	0.0	−14.0	28.1	27.1	0.3	−1.9
84	210	0.56	0.0	−11.8	24.7	23.6	1.4	−1.9
84	212	0.53	0.47	−9.9	22.9	22.0	1.3	−1.8
86	210	0.76	0.21	−8.5	19.7	18.3	3.9	−2.8
86	212	0.73	0.0	−9.9	21.2	20.3	2.6	−1.5

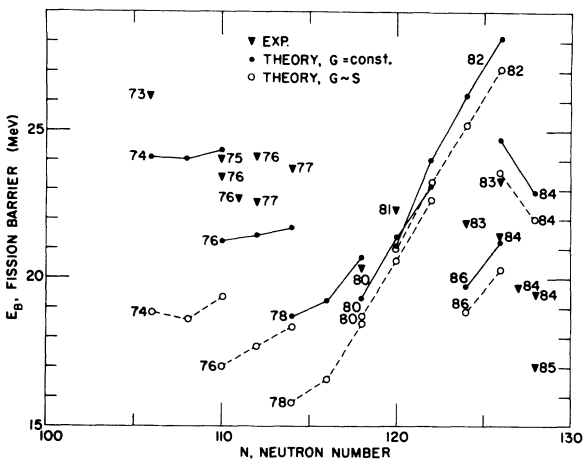

FIG. 5. Comparison of calculated fission-barrier heights both for the pairing strength G = const. and $G \sim S$ with experimental numbers. No zero-point energies have been taken into account in this comparison. The experimental values are those of Moretto *et al.* (Ref. 14) and have an uncertainty of ±1 MeV (Ref. 14). The numbers in the figure give the charge numbers Z of the nuclei.

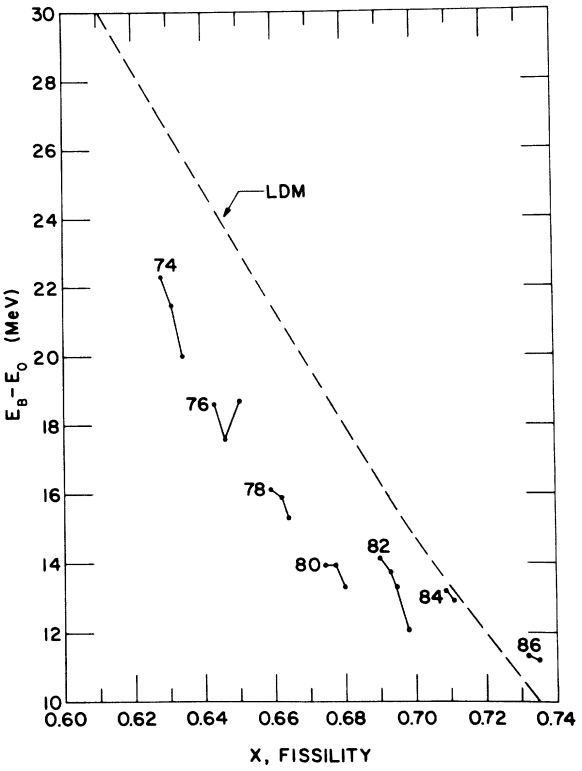

FIG. 6. Plot of the energy difference $E_B - E_0$, where E_B is the calculated barrier energy and E_0 the ground-state energy shell correction $(\delta U + E_p)$. The dashed line shows the LDM barrier heights.

The origin of this structure will be discussed later in Sec. III D. For the present purpose it is enough to notice that the LDM saddle point lies in the shell-correction valley and that the saddle is shifted towards smaller constrictions.

The observed lowering of the fission barriers under the LDM value is in all cases the consequence of the always negative pairing energy and of the valley in the energy shell correction. This valley, which is rather weakly developed in the region around $A = 180$, increases in strength toward $A = 200$ and then slowly shifts towards larger l values around $A = 210$ and thus away from the LDM saddle.

This appearance of a rather strong negative shell correction at the saddle is of great importance for the evaluation of level densities at the saddle point and for the determination of nuclear mass formulas as has already been mentioned above.

Since it has been assumed in all recent mass formulas in which experimental fission barrier energies have been used for a determination of the parameters[11,16] that no energy shell corrections exist at the barrier, these fits may have resulted in a wrong decomposition of the saddle-point mass into a LDM and a shell contribution. Such a wrong decomposition then affects, of course, the determination of the LDM parameters. It should be remembered that the existence of pairing condensation energies and of shell corrections throughout

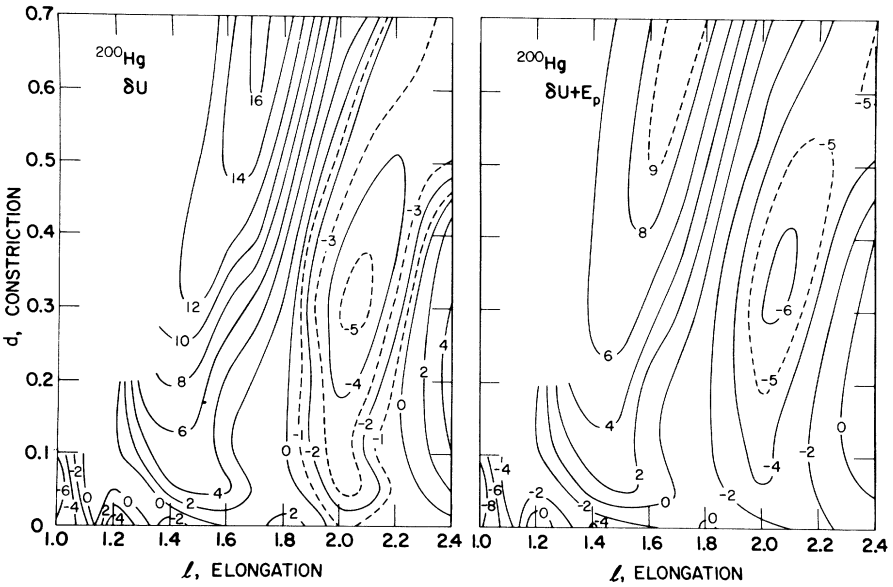

FIG. 7. Contour plots of energy surfaces for ^{200}Hg. The left half of this figure shows the pure shell correction δU, the right part the total energy shell-correction surface $(\delta U + E_p)$.

the Periodic Table and for rather large ranges of deformation is the rule and not the exception. One would, therefore, *a priori* expect the existence of single-particle effects also at the saddle.

A further consequence of the existence of shell effects at the saddle would be an uncertainty in the experimental barrier energies of Morreto *et al.*[14] For the determination of these barriers from the measured excitation energy dependence of Γ_f/Γ_n, the level densities at the barrier have to be known. For the experimental numbers quoted above, the *a priori* assumption of a uniform level density at the saddle has been made thus again minimizing possible shell effects at the saddle. This assumption may have influenced the experimental barrier energies.

Up to now only the Los Alamos group of Nix *et al.*[2] has calculated barriers in this mass region, namely, for the two cases ^{188}Os and ^{210}Po. These authors as well as all others listed in Ref. 2 have used for their calculations a finite-depth single-particle potential. The advantage of using such a potential as compared to a harmonic-oscillator model like the one presented here, however, is lost as far as the finite depth is concerned: This is so because in all calculations of shell corrections in finite-depth potentials made to date[2], the continuum states in the Strutinsky smearing procedure have been replaced by an artifact, usually the bound states that appear at energies $E > 0$ in the diagonalization of a finite-depth potential in a harmonic-oscillator basis which has been used in all these calculations. These states, however, all converge to zero energy with increasing basis dimensions.[8] In a very comprehensive study it has been shown by Nix *et al.*[2] that thus in these models the shell correction, calculated with the Strutinsky prescription,[2] depends even on the size of the basis used. The only essential difference that remains then between the use of a finite depth and an infinite potential is not the more realistic finite depth, but the better description of the nuclear surface region in the former one. This makes the use of the rather ambiguous $\hat{l}^2$ term of the oscillator models unnecessary.

In spite of this difference, the two fission barriers calculated by Nix *et al.* agree with the present theoretical results remarkably well. This and the disagreement with experiment of both calculations for ^{210}Po seems to indicate a model-independent, rather general difficulty in this mass region especially in view of the excellent agreement reached in the actinide region.[1,2]

C. Fission-Barrier Heights, $G \sim S$

Since there have been both theoretical[17] and experimental[18] suggestions that the pairing strength might be a function of the surface area, all calculations reported above also have been done with a pairing strength proportional to the nuclear surface. The results for the barriers are also listed in Table I and one example of the PES is shown in comparison with that corresponding to $G = \text{const.}$ in Fig. 9.

In the lighter elements especially, the barrier energies are drastically decreased, by up to 5 MeV, compared with the results obtained with a

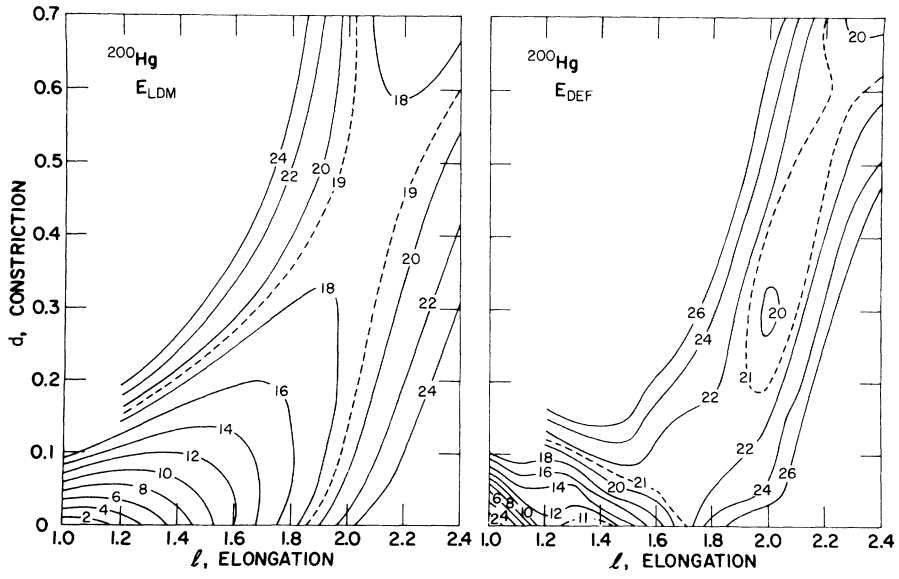

FIG. 8. Contour plots of energy surfaces for ^{200}Hg. The left part of the figure shows the LDM PES, the right part the total PES.

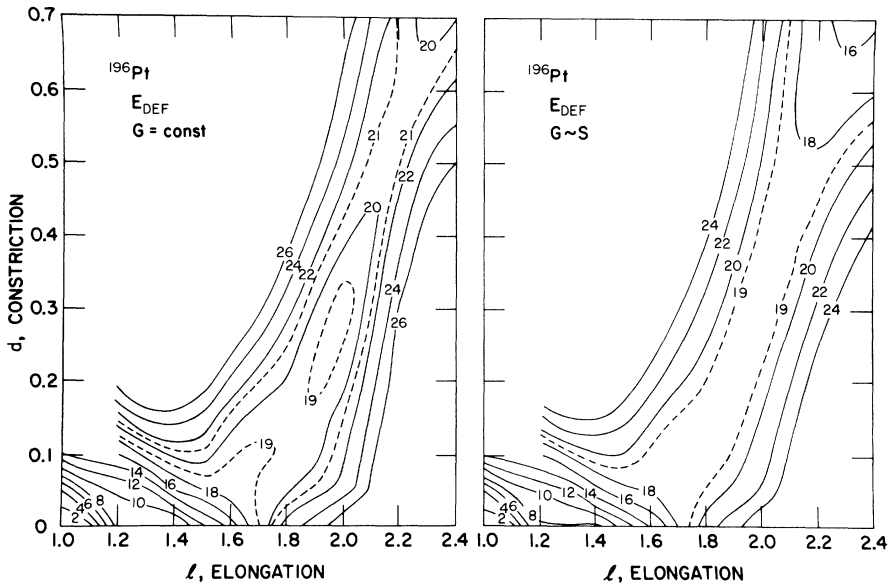

FIG. 9. The total PES's calculated with a surface-dependent pairing strength (right) and with a constant pairing strength (left) are compared for the nucleus ^{196}Pt. For other details see Fig. 2.

constant strength, whereas the suppression is rather small (≈1 MeV) for the nuclei around Pb.

The effect of the assumption $G \sim S$ is in general appreciably larger than, for example, in the actinides because of the much larger surface area at the saddle for these lighter nuclei. These nuclei, therefore, constitute a better test for the assumption of a surface-dependent pairing strength. The reason for the relatively small effect in the Pb, Po region reflects the fact that here the saddle points appear already at rather small deformations (see Fig. 4).

A natural by-product of these calculations is the gap parameters Δ in the BCS formalism. The conclusion that the experimental angular distributions of fission products of ^{210}Po indicated a pairing strength larger at the saddle than at the ground state were based on the observation of a very low variance of the K quantum number at the saddle. This was interpreted as being due to an abnormally large gap there.[18] A comparison of the theoretical gaps at the saddle-point deformation for both G= const. and $G \sim S$ is, therefore, given in Table III for the case of ^{198}Hg (Natowitz and Chulick[19]) and for ^{210}Po. It is seen that in these two nuclei both the proton and the neutron gaps increase by going from the ground state to the saddle by about a factor of 1.5 for $G \sim S$, whereas they stay practically constant for G = const. (The apparent strong increase of Δ_n in the case of ^{210}Po is a trivial consequence of the strong neutron shell at the spherical ground state.) The increase for $G \sim S$ is much smaller than the change the anisotropy experiment seems to indicate (factor of 2–3).[18] It should here also be noted that an experiment similar to that of Ref. 18 for ^{210}Po has been performed by Kuvatov, Okolovich, and Smirenkin[19] for the two nuclei ^{208}Po and ^{212}Po. In these two cases no anomaly in the anisotropies at low excitation energies has been observed.

We see, therefore, that the assumption of a pairing strength proportional to the nuclear surface and increasing with it leads, on the one hand, to fission barriers in the lighter nuclei that are too small by about 6 MeV, and on the other hand to gaps which are not sufficiently large to explain the observed anisotropy. We thus conclude that the assumption of a pairing strength directly proportional to the nuclear surface area is incompatible with experimental data on fission-barrier heights.

TABLE III. For the two nuclei given the table lists the BCS gap parameters both for a constant and a surface-dependent pairing strength G. The gap parameters are given separately for protons and neutrons (p, n) and both for the ground state (gs) and the saddle point (sp) as calculated in this paper. All gap parameters are given in MeV. The corresponding experiments have been performed by Moretto *et al.* (Ref. 18) and Natowitz and Chulick (Ref. 19).

			G = const.		$G \sim S$	
Nucleus	$\Delta_{p,\mathrm{gs}}$	$\Delta_{n,\mathrm{gs}}$	$\Delta_{p,\mathrm{sp}}$	$\Delta_{n,\mathrm{sp}}$	$\Delta_{p,\mathrm{sp}}$	$\Delta_{n,\mathrm{sp}}$
^{210}Po	0.56	0.0	0.63	0.61	1.00	1.01
^{198}Hg	0.49	0.74	0.59	0.56	1.12	0.94

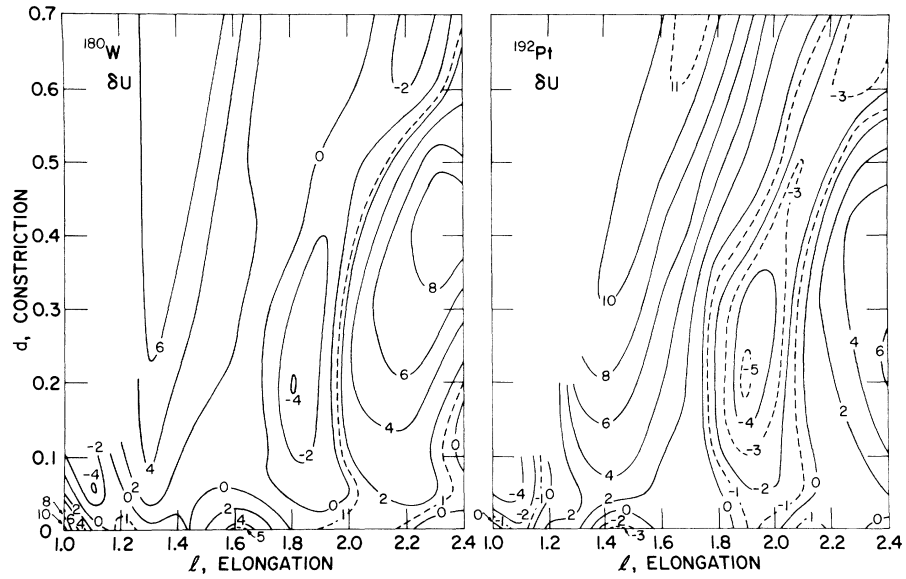

FIG. 10. The shell-correction surfaces are shown for ^{180}W (left) and ^{192}Pt (right).

D. Structure of the Energy Shell Corrections

As has been discussed briefly in Sec. III B, the calculated fission barriers are lower than the values given by a LDM that is corrected for the ground-state shell effect. It has been shown that this lowering of the barrier is due to the pairing energy and to a pronounced valley-like structure in the energy shell correction. In this paragraph we will, therefore, investigate the origin of this structure that is well-developed in all nuclei calculated here, that has also been observed, though at a different deformation, in the actinides,[7] and that is thus a very general phenomenon.

In Figs. 7 and 8 four contour plots are shown giving the LDM PES, the shell-correction surface, the total energy-shell correction, $\delta U + E_{\mathrm{p}}$, and the total PES, E_{DEF}, for ^{200}Hg. It is seen that the structure in the energy shell correction is due to the δU behavior alone and that the pairing contribution, because it counteracts the shell correction, only smooths the shell-correction surface to a certain extent.

In order to show the dependence of these structures in δU on the mass of the fissioning compound nucleus, the shell-correction surfaces are given in Figs. 10 and 11 for ^{180}W, ^{192}Pt, and ^{210}Po. These diagrams together with Fig. 7 show very well the gradual shift of the valley from $l \approx 1.8$ up to $l \approx 2.2$, its deepening from ≈ -4 MeV at $A = 180$ to ≈ -5 MeV in ^{198}Hg (see Fig. 7) and a stabilization of the structure in the region $A \approx 212$. At the same time it is noticeable that these valleys usually do not run continuously out to smaller energies but are deepest at small constrictions ($d \approx 0.2$), go over a slight maximum at $d \approx 0.5$, and then decrease again or, in the heaviest elements considered here, do not decrease any more from here on. This behavior indicates that a discussion of this structure in terms of fragment shell effects alone which is suggested by the fact that these valleys run out towards scission essentially along the constriction

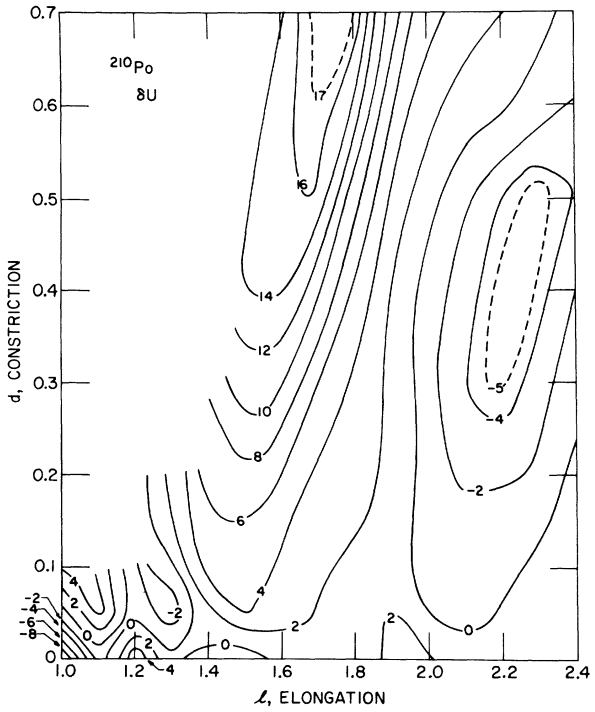

FIG. 11. The shell-correction surface is shown for the nucleus ^{210}Po.

degree of freedom may be too simplifying.

An analysis of the single-particle levels at $d \approx 0.5$ shows that states with the same projection of the angular momentum on the nuclear symmetry axis but different parity are practically degenerate with this degeneracy broken at the Fermi surface by less than 1 MeV. This means that these states are already highly localized in either one of the two fragments.[20] The structure at large constrictions ($d \gtrsim 0.5$) thus is to a large extent due to fragment shell effects. In order to corroborate this point we show in Fig. 12 $\delta U(l)$ corresponding to cuts at $d = 0.5$ through the δU planes in comparison with the prediction of a two-spheroid scission model consisting of two noninteracting Nilsson models with the same elongation l and using the same single-particle parameters κ and μ (see also Mosel and Schmitt[7]). The general behavior of these curves can be understood by observing that the fragments lie in a transition region between spherical and permanently deformed nuclei. They have thus first only a small change in δU when going from the spherical shape ($l \approx 1.6$) to the deformed one ($l \gtrsim 1.6$) ($\approx$2.5 MeV in ^{92}Sr) with this difference increasing with increasing mass when the deformed shell is more strongly developed ($\approx$7.6 MeV in ^{106}Mo).

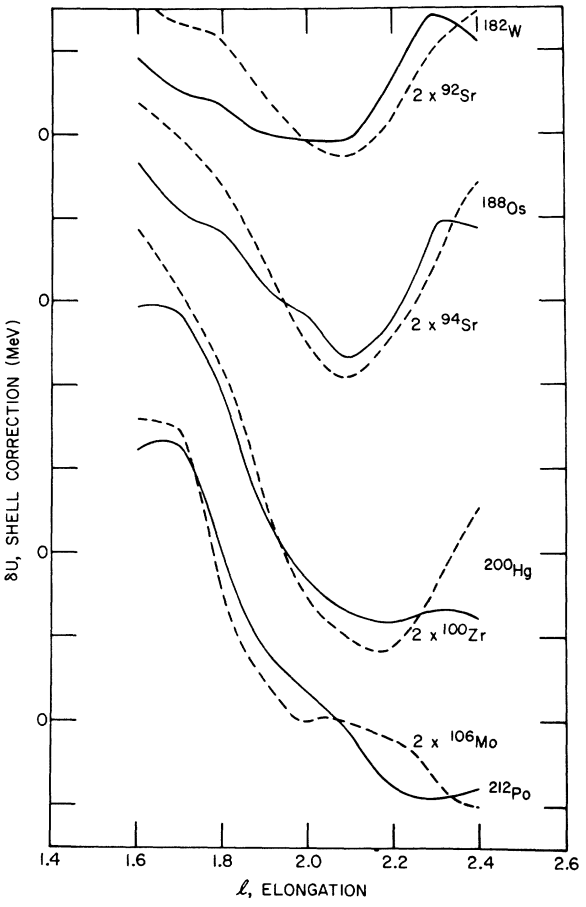

FIG. 12. The shell correction δU is shown as a function of the elongation l at $d = 0.5$ (solid lines) in comparison with the prediction of a two-spheroid *scission* model (dashed curves). The nuclei indicated in the figure give the compound nuclei (solid lines) and the corresponding pairs of fragments (dashed lines). The positions of zero shell correction for each nucleus are given on the δU axis in vertical order. The separation between two marks on this axis is 5 MeV.

The remarkable agreement between these two models both as a function of mass as well as of elongation indicates that at these constrictions the shell corrections are to a very large extent due to the fragment shell structure. The Figs. 7, 10, and 11 show, however, that the structures in the δU surfaces appear already at very small constrictions ($d \approx 0.0$–0.05). This cannot be a consequence of the fragment shells, since at small d's the single-particle potentials are essentially one-centered potentials and thus describe only the shells of the fissioning system.

The question then arises how can one understand the appearance of the dominant structures in the δU surfaces parallel to the constriction axis and especially their very early onset with constriction. The answer to this question lies in the special deformation dependence of nuclear shells. It has been shown by Geilikman,[21] Myers and Swiatecki,[22] and especially in great detail by Wong[23] that in pure deformed harmonic-oscillator model shells, i.e., zones of low single-particle level density at the Fermi surface, appear when the ratio of axes of the nucleus is that of two integer numbers. These simple shells can also be identified, though perhaps somewhat shifted, in more sophisticated potentials like the Nilsson or Woods-Saxon potential.[23] The actual influence of these deformed shells on the nuclear structure depends, of course, also on the proton and neutron numbers which determine if a given shell is indeed populated. In Wong's[23] notation the (1 : 1) shell is responsible for the existence of spherical nuclei, the ground states of the deformed rare earths and actinides are due to the (3 : 4) shell, the fission isomeric minima in the actinides originate in the (1 : 2) shell, and the (2 : 3) shell is responsible for the appearance of second minima in the Pb region (see, for example, Fig. 3 at $d = 0$, $l = 1.4$ and discussion of this point in Sec. III E).

These ratios of the semiminor to the semimajor axis of the spheroidal nucleus ($m : n$) can easily be converted into the elongation parameter l. One obtains $l_c = (n/m)^{2/3}$ for a given deformation of the compound nucleus. One sees, for example, by an inspection of the δU surface for ^{200}Hg (see Fig. 7) that on the $d = 0$ axis minima in δU appear at $l = 1.0$,

$l \approx 1.40$, and $l \approx 2.1$ corresponding to the shells (1:1), (2:3), and (1:3).

It is obvious from Fig. 7 that the (1:3) shell appears at $d=0$ at the same elongation l as fragment shells appear at $d \approx 0.5$. The fragment and compound-nucleus shell effects in this case are thus in the (d, l) plane aligned.

The reason for this remarkable behavior can be understood in a model in which the scission configuration is approximated by that of two equal noninteracting touching spheroidal nuclei, each of them described by, e.g., a Nilsson model. The fragment shell effects lead to local minima in the dependence of the total energy at scission as a function of elongation at deformations close to one of the values $(m:n)$ listed above.

It can easily be calculated that these favorable elongations of the fragments correspond to $l_F = (2n/m)^{2/3}$ (l is the total elongation relative to the radius of the *fissioning* nucleus). This means that the fragment shells and those of the fissioning nucleus can only appear in line, i.e., for the same l, if $l_c = l_F$. This can only be fulfilled for two cases: The (1:1) and the (2:3) fragment shells coincide with the (1:2) and the (1:3) compound shells, respectively.

The present calculations show that of these two only the (1:3) compound shell at $l \approx 2.1$ is actually effective in the Pb region. At the same time the (2:3) shell in the fragment region is dominant.

This latter shell actually is responsible for the existence of a new region of deformed nuclei around $A \approx 100$.[24] This may be the reason why these nuclei show even larger ground-state deformations than the rare earths corresponding to the less deformed shell (3:4).

This alignment of fragment and compound shells explains the observed structures in δU and their nearly exclusive d dependence: Fragment shell effects reach in from scission to smaller constrictions, whereas compound shells reach out at the same elongation towards larger constrictions, meeting each other halfway. The appearance of a local maximum in the δU valley at $d \approx 0.5$ is a consequence of this special behavior. The ridge in δU observed in all nuclei is a consequence of the antishell in the fragments at $l \approx 1.59$ (1:1 shell) corresponding to a positive shell correction at the spherical shape of these permanently deformed fragment nuclei.

The slight bending of the δU valleys towards larger d's starting at $d \approx 0.4$–0.5 is a consequence of the fact that the actual scission configuration in the shape parametrization used here is longer than that of two corresponding touching spheroids with this extra length increasing with d. A better simulation of the true scission configuration would thus be given by two spheroidal fragments whose surfaces are separated by a certain distance. This, however, does not affect the comparison of the δU's presented above which has been made at $d=0.5$.

A further analysis of the shell corrections δU in the valley shows that they originate mainly in the neutron shell structure with the neutrons contributing approximately 60–70% of the total shell correction. This might be due to the fact that in the fragments formed ($Z_F \approx 40$, $N_F \approx 60$) the protons are close to a magic number, whereas the neutrons are located more in the middle of a shell thus favoring deformed shapes.

E. Local Minima in the PES Below the Barrier

As already mentioned briefly in Sec. III D, the (2:3) shell is populated in some of the nuclei in the Pb region thus leading to a second minimum in the total PES at $d=0$ and $l \approx 1.4$ (see, e.g., Fig. 3). For a few cases these secondary minima had already been observed.[7,25]

The present results show that these minima appear for all nuclei above $A=198$, first in ^{198}Hg at 9-MeV excitation energy, then, due to the increasing shell effect at the ground state, the minima increase in energy up to 17.1 MeV in ^{208}Po and decrease again to 13.4 MeV in ^{212}Rn. These excitation energies, taken together with the barrier energies, show that the propability for possible states in these minima to decay by fission is vanishingly small because of the high and broad barrier which has to be penetrated. Instead – if these states can be populated at all – delayed γ decay or neutron emission should be the predominant decay channels. An experimental search for delayed γ rays of about 10 MeV should be initiated in these nuclei.

F. Local Minima in the PES at the Barrier

Figures 3, 4, 8, and 9 show that besides the minima mentioned above in Sec. III E minima also appear on top of the fission barrier if a constant pairing strength is used for all deformations. These minima exist around the nucleus ^{198}Hg and have a depth of about 2 MeV. They are a consequence of the rather broad and flat LDM barrier in this region (see Fig. 3) and the existence of the energy correction valley at $l \approx 2.0$ which counteracts the increase of the LDM barrier and thus flattens the total barrier even more. It is, of course, possible that in these nuclei shell effects at the barrier may lead to structures similar to those in the actinides which are there responsible

for the existence of fission-isomeric states. The difference between the two mass regions lies only in the fact that for $A \approx 200$ the barriers and thus the minima on top of them appear at higher energies and larger constrictions (see Fig. 13) than in the actinides. This might suggest an interpretation of states in these minima as "quasimolecular" states. (The term quasimolecular state is used here to indicate a metastable configuration consisting of two, to a large extent preformed, nascent fragments; this definition does not necessarily imply a separation between these two fragments.)

One should be aware, however, of the possibility that these local minima might be a consequence of a special shape parametrization. Nevertheless, it will be interesting to look for these structures in other independent calculations that might soon become available.

IV. INFLUENCE OF ZERO-POINT ENERGIES ON BARRIER HEIGHTS

In all the interpretations discussed above, the zero-point energy has been completely neglected in contrast to calculations of other authors who chose to subtract an arbitrary number (usually about 0.5 MeV) from the calculated fission-barrier heights in order to take the change in zero-point energies between the ground state and the saddle into account (see, e.g., Nix *et al.*[2] and Nilsson *et al.*[1]).

The problem here consists in determining the *difference* between the zero-point energies at the saddle and the ground state, ΔE_0, since the measured barrier is given by $E_B + \Delta E_0$. Here E_B is the energy difference between the *static* saddle point and the static ground state as calculated from Eq. (6).

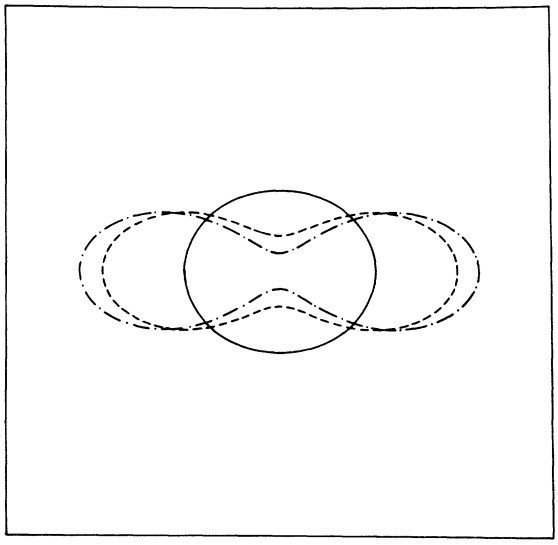

FIG. 13. For the nucleus ^{192}Pt the shapes at the ground state (solid line), at the saddle point (dashed line), and at $l = 2.4$, $d = 0.7$ (dot-dashed line) are shown.

The nuclear mass formula (LDM + shell correction) has been fitted to the experimental ground-state masses which, of course, already contain the effects of the zero-point energy, by identifying the energy surface minimum with the experimental mass. It is, therefore, evident that the ground-state minima in the energy surfaces calculated as described above do not represent *potential* minima but do give directly the energy of the ground state with the zero-point energy included. (In this sense, therefore, the term *potential* energy surface is misleading.) As far as a calculation of the absolute mass is intended, therefore, no additional zero-point energies may be added.

For the saddle point obviously a similar argument would hold: *If in a fit of the mass formula, experimental values of fission barriers as well as ground-state masses have been used, then no additional corrections to the barriers due to the zero-point energies may be added.* This is so because again the experimentally measured barrier energies already contain all zero-point energy effects. The question then is if and how the conditions mentioned above are taken into account in commonly used mass formulas.

Myers and Swiatecki[11] have indeed used one experimental barrier height in their mass formula, namely, that of ^{201}Tl with the assumption of no shell effects at the saddle. This means that for this one nucleus ^{201}Tl at least a part of the saddle zero-point energy, namely, that originating in the LDM, has implicitly been taken into account.

The conclusion from above is that one should *not* take additionally into account zero-point energies if one is working with a mass formula that has been explicitly fitted to the experimental ground-state *and* barrier energies in that particular mass region in which one is working. At least in a first approximation this is the case for the Myers and Swiatecki mass formula for the nucleus ^{201}Tl and presumably also other nuclei not too far away. In this sense Figs. 2–4 and 8 should not be considered as *potential* energy surfaces but as energy surfaces which pass at the stationary points through the energies of the lowest possible quantum-mechanical states.

This conclusion, however, is in principle true only for the calibration nucleus ^{201}Tl and depends on the tacit assumption that these zero-point energies behave smoothly with mass. It, therefore, cannot directly be generalized to other mass regions. Especially in the region of superheavy nu-

clei, far away from the calibration nucleus ^{201}Tl, zero-point energies may have an important influence on the effective barrier heights and thus the lifetimes of these elements as has already been discussed elsewhere.[3,26]

V. SUMMARY AND CONCLUSIONS

Calculations of fission barriers in the mass region $180 \leq A \leq 212$ have been presented for 20 even-even nuclei in the framework of the symmetric TCM. Except for two earlier preliminary and incomplete attempts (Nix *et al.*[2] and Mosel and Schmitt[9]), these calculations represent the first theoretical approach to a determination of the saddle points and the ground state in this mass region on the same basis.

A. Shell Corrections at the Saddle

The calculations have consistently led to negative shell corrections at the barrier thus casting some doubt on the implicit assumption of recent mass-formula fits that no shell effects exist at the saddle. It was pointed out that because of the rather widespread appearance of shell effects there is no *a priori* reason why these should be nonexistent at the barriers around $A \approx 200$. The neglect of shell effects at the saddle may have led to a wrong decomposition of the saddle-point mass into the LDM and the shell-correction part thus influencing the determination of the LDM parameters.

B. Barrier Heights

Although in view of the exploratory character of this calculation, the agreement with experiment is quite satisfactory, the calculated barriers for $A \lesssim 200$ are found to *underestimate* the experimental fission barriers. This may be partly due to the reasons mentioned above and to an imperfect description of the pairing energies at the saddle which are essentially counted twice because they are implicitly already included in the LDM that has been fitted to an experimental barrier height. Since here the calculated barriers are usually too *low*, the discrepancy cannot be attributed to non-optimal nuclear shapes. It is worthwhile to mention that the only independent calculations of barriers for two nuclei in this region by Nix *et al.* agree well with the present theoretical values and thus disagree as much as the latter with the experimental barrier height of ^{210}Po.

C. Surface Dependence of the Pairing Strength

Since the fission barriers in the mass region considered in this paper are considerably more deformed than those in the actinides, the results for the nuclei around $A \approx 200$ are more sensitive to a surface dependence of the pairing strength. All calculations have, therefore, been performed both with a surface-dependent and a constant pairing strength. The assumption of a pairing strength directly proportional to the surface area of the nucleus, leads to a lowering of the fission barrier by about 5 MeV compared with the value obtained with a constant G that describes the experimental barrier height reasonably well. At the same time, the BCS gaps increase from the ground state to the saddle only by about a factor of 1.5 instead of the experimentally postulated factor of 2–3 in ^{210}Po.[18]

The conclusion thus is that the assumption of a pairing strength proportional to the surface area of the nucleus is incompatible with the experimental data on fission-barrier heights and transition-state properties.

D. Connection Between Fragment and Compound-Nucleus Shells

An analysis of the shell corrections alone has shown that these reveal remarkable structures which are due to an interplay between shells of the fissioning nucleus and those of the two fragments. It was especially pointed out that for specific particle numbers shells in the compound nucleus appear at the same geometrical configuration as those of the fragments thus explaining the onset of structures (valleys and ridges) in δU at very small constrictions and their much stronger dependence on the elongation than on the constriction degree of freedom.

E. Zero-Point Energies

Finally the treatment of the zero-point energy and its influence on the theoretical determination of fission barriers was discussed. It was argued that in a model in which *both* experimental ground-state and fission-barrier masses have been used for a mass-formula fit, no additional zero-point energies should be added in the calculations because they are contained already in the experimental masses. The mass formula most widely used in these calculations, namely that of Myers and Swiatecki, has indeed used the experimental fission barrier of ^{201}Tl in its fit, though without inclusion of shell effects at the barrier. Nevertheless this mass formula should at least in a first approximation be considered to contain the effects of the zero-point energies when used around $A \approx 200$. In other mass regions, however, and especially in the region of superheavy nuclei, this assumption may not be true any more so that there the inclusion of the difference between the zero-

point energies can lead to drastic changes in the effective fission barriers and lifetimes.

It is furthermore clear from these considerations that energy surfaces calculated by using a shell-correction method on the basis of an empirical LDM may not be used in a quantum-mechanical calculation, since they already contain the zero-point energies.

ACKNOWLEDGMENTS

I would like to acknowledge stimulating discussions concerning this work with many of my colleagues in this field. In particular, I have greatly benefitted from numerous helpful and encouraging discussions with H. W. Schmitt in the early stages of this work. His suggestions and comments have had a major impact on this work. I am also highly obliged to R. Vandenbosch for his vivid interest in these calculations and the numerous thorough discussions we had on this subject. I also wish to thank him for a careful reading of the manuscript and many helpful comments on it. I would finally like to acknowledge several clarifying discussions with L. Wilets, especially on the problem of the treatment of zero-point energies.

---

*Work supported by the U. S. Atomic Energy Commission.

[1]S. G. Nilsson *et al.*, Nucl. Phys. A131, 1 (1969); P. Möller, to be published, and references therein; see also Ref. 4.

[2]V. M. Strutinsky, Nucl. Phys. A95, 420 (1967); A122, 1 (1968); M. Bolsterli, E. O. Fiset, J. R. Nix, and J. L. Norton, Phys. Rev. C 5, 1050 (1972); V. V. Pashkevich, Nucl. Phys. A169, 275 (1971); V. M. Strutinsky and H. C. Pauli, in *Proceedings of the Second International Symposium on the Physics and Chemistry of Fission, Vienna, Austria, 1969* (International Atomic Energy Agency, Vienna, Austria, 1969), p. 155; H. C. Pauli, T. Ledergerber, and M. Brack, Phys. Letters 34B, 264 (1971); H. C. Pauli and T. Ledergerber, Nucl. Phys. A175, 545 (1971).

[3]U. Mosel and W. Greiner, Z. Physik 222, 261 (1969).

[4]T. Johansson, S. G. Nilsson, and Z. Szymanski, Ann. Phys. (Paris) 5, 377 (1970).

[5]P. Holzer, U. Mosel, and W. Greiner, Nucl. Phys. A138, 241 (1969); D. Scharnweber, W. Greiner, and U. Mosel, *ibid.* A164, 257 (1971); B. L. Anderson, F. Dickman, and K. Dietrich, *ibid.* A159, 337 (1970); C. Y. Wong, Phys. Letters 30B, 61 (1969).

[6]U. Mosel and H. W. Schmitt, Nucl. Phys. A165, 73 (1971).

[7]U. Mosel and H. W. Schmitt, Phys. Rev. C 4, 2185 (1971); U. Mosel and D. Scharnweber, Phys. Rev. Letters 25, 678 (1970).

[8]M. Bolsterli *et al.*, Ref. 2.

[9]U. Mosel and H. W. Schmitt, Phys. Letters 37B, 335 (1971).

[10]L. A. Malov, V. G. Soloviev, and I. D. Khristov, Yadern. Fiz. 6, 1186 (1967) [transl.: Soviet J. Nucl. Phys. 6, 863 (1968)]; D. A. Arseniev, A. Sobiczewski, and V. G. Soloviev, Nucl. Phys. A139, 269 (1969).

[11]W. D. Myers and W. J. Swiatecki, Arkiv Fysik 36, 343 (1967); and private communication (computer code LYMASS).

[12]S. G. Nilsson, Kgl. Danske Videnskab. Selskab. Mat.-Fys. Medd. 29, No. 16 (1956); U. Mosel and W. Greiner, Z. Physik 217, 256 (1968); D. Bès and Z. Szymanski, Nucl. Phys. 28, 42 (1961).

[13]See, e.g., Nucl. Data B1, No. 1 (1966).

[14]L. G. Moretto, S. G. Thompson, J. Routti, and R. C. Gatti, Phys. Letters 38B, 471 (1972).

[15]V. S. Ramamurthy, S. S. Kapoor, and S. K. Kataria, Phys. Rev. Letters 25, 386 (1970).

[16]P. A. Seeger, Los Alamos Scientific Laboratory Report No. LA-DC-12792, 1971 (unpublished).

[17]R. C. Kennedy, L. Wilets, and E. M. Henley, Phys. Rev. Letters 12, 36 (1964).

[18]L. G. Moretto *et al.*, Phys. Rev. 178, 1845 (1969).

[19]J. B. Natowitz and E. T. Chulick, Nucl. Phys. A172, 185 (1971); K. G. Kuvatov, V. N. Okolovich, and G. N. Smirenkim, Zh. Eksperim. i Teor. Fiz. Pis. Red. 11, 42 (1970) [transl.: Soviet Phys.–JETP Letters 11, 26 (1970)].

[20]If two states with different parity but identical in all other quantum numbers and in energy are linearly combined, they have still the same eigenvalue but are localized in either one of the two fragments: See Ref. 6 for a discussion of this point.

[21]T. Geilikman, in *Proceedings of the International Conference on Nuclear Structure, Kingston* (Toronto U. P., Toronto, 1970), p. 874.

[22]W. D. Myers and W. J. Swiatecki, unpublished work, private communication.

[23]C. Y. Wong, Phys. Letters 32B, 668 (1970); and to be published.

[24]E. Cheifetz, R. C. Jared, S. G. Thompson, and J. B. Wilhelmy, Phys. Rev. Letters 25, 38 (1971).

[25]C. F. Tsang and S. G. Nilsson, Nucl. Phys. A140, 275 (1970).

[26]J. Grumann, U. Mosel, B. Fink, and W. Greiner, Z. Physik 228, 371 (1969); *Proceedings of the Robert A. Welch Foundation Conferences on Chemical Research, XIII, The Transuranium Elements, Mendeleev Centennial, Houston, 1969* (Robert A. Welch Foundation, Houston, Texas, 1970), pp. 206–211.